Akademia Górniczo-Hutnicza
im. Stanisława Staszica w Krakowie

AGH University of Krakow

Toward Precision Helicity PDFs from Global DIS and SIDIS Fits with Projected EIC Measurements

Hamzeh Khanpour, Maryam Soleymaninia, Majid Azizi, Michael Klasen, Hadi Hashamipour, Maral Salajegheh, and Ulf-G. Meißner

arXiv:2602.17298 [hep-ph]; to appear in Phys. Rev. D

DIS 2026, Bologna, 7 May 2026

Outline

1. Physics motivation and analysis scope
2. Theory framework and data input
3. Fit methodology and stability
4. Impact of projected EIC SIDIS data on helicity PDFs
5. Comparison to recent global fits
6. Physics outcomes and implications

Proton spin puzzle and why helicity PDFs still matter

- A central QCD question is how the proton spin is shared among quark helicity, gluon helicity, and orbital angular momentum.
- The EMC result showed that quark spin alone accounts for only a limited fraction of the proton spin.
- Helicity-dependent PDFs, $\Delta q(x, Q^2)$ and $\Delta g(x, Q^2)$, are the basic collinear objects that connect polarized scattering data to the proton spin decomposition.
- Their lowest moments enter, schematically, the longitudinal spin decomposition:

$$\frac{1}{2} = \frac{1}{2}\Delta\Sigma(Q^2) + \Delta g(Q^2) + L_q(Q^2) + L_g(Q^2).$$

- The main missing information is concentrated in poorly constrained flavor separation and in the small-x region.

Talk focus

From a global DIS+SIDIS fit we ask: how much can projected EIC SIDIS data improve

- sea-quark flavor separation,
- the small-x behavior of helicity PDFs,
- the strange sector, especially Δs and $\Delta\bar{s}$,
- the gluon helicity uncertainty through the extended Q^2 lever arm,
- the stability of the extraction against SIDIS cuts such as $z_{\min}$,
- and the quark+gluon spin contribution?

The Electron-Ion Collider (EIC): a QCD microscope for spin and structure

What is the EIC

A high-luminosity electron-ion collider at BNL, designed for variable-energy ep and eA collisions, with polarized electron and polarized proton/light-ion beams.

Why it is unique for spin physics

The combination of polarization, collider kinematics, and high luminosity gives direct access to spin-dependent structure functions, helicity PDFs, and the poorly constrained small-x spin sector.

Broader QCD program

Beyond helicity PDFs, the EIC addresses 3D nucleon tomography, gluon saturation, nuclear PDFs, fragmentation, hadronization, and proton PDFs/α_S.

See talk by Katarzyna Wichmann

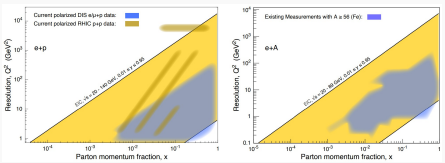

EIC $e+p$ reach in the (x, Q^2) plane compared with existing polarized data.

Connection to this talk

For helicity PDFs, the decisive gain comes from combining inclusive polarized DIS with identified-hadron SIDIS:

$$g_1 \Rightarrow \Delta\Sigma,\ \Delta g, \qquad A_1^h \Rightarrow \Delta\bar{u},\ \Delta\bar{d},\ \Delta s,\ \Delta\bar{s}.$$

The EIC will extend polarized DIS and SIDIS measurements into a much wider (x, Q^2) region, making the small-x and sea-flavor helicity PDFs far more data-driven than in present fixed-target analyses.

Why EIC? Why small x? Why SIDIS?

- Existing fixed-target polarized DIS and SIDIS data provide important constraints at moderate and large x, but the small-x region remains extrapolation-dominated.
- Inclusive DIS is essential for the quark singlet and, through scaling violations, for Δg.
- SIDIS adds flavor tagging through identified hadrons:
  - $\pi^{\pm}$ channels sharpen sensitivity to $\Delta\bar{u}$ and $\Delta\bar{d}$,
  - $K^{\pm}$ channels provide unique leverage on Δs and $\Delta\bar{s}$.
- The EIC extends the accessible (x, Q^2) region, giving both lower x reach and a stronger multi-scale lever arm.
- In our setup this means projected sensitivity down to roughly $x \sim 10^{-5}$ from SIDIS pseudodata at two beam configurations.

Main physics point

The EIC is not simply a source of more precise data: it qualitatively strengthens the constraining power of SIDIS in the poorly known small-x and sea-quark sectors.

Refs: Borsa et al., Phys. Rev. D 102 (2020) 094018; ECCE detector Nucl. Instrum. Meth. A 1056 (2023) 168563

How this analysis is positioned in the current literature

Present-data global benchmarks

- BDSSV24/DSSV: NNLO global benchmark with DIS, SIDIS, and RHIC pp spin asymmetries from $W^{\pm}$, hadron, and jet production.
- JAMpol25/JAMsmall-x: NLO global spin-PDF program with high-x, higher-twist, plus distinct small-x helicity-evolution studies.
- MAPPDFpol1.0: NNLO DIS+SIDIS, neural-network Monte Carlo methodology, positivity studies, and FF-dependent flavor separation.
- NNPDFpol2.0: NNLO DIS+$W^{\pm}$+jets+dijets fit with modern ML methodology, positivity studies, and theory covariance; no direct SIDIS input.

Our niche in this talk

- Deliberately restricted DIS+SIDIS baseline.
- Explicit focus on projected EIC SIDIS pseudodata.
- NLO, leading-twist, collinear framework.
- Monte Carlo replicas + neural-network parametrization.
- Main emphasis on sea-quark flavor separation and small-x impact.

Representative references

- BDSSV24/DSSV: PRL 133 (2024) 151901;
- JAMpol25/JAMsmall-x: PRD 112 (2025) 114017, PRD 108 (2023) 114007, arXiv:2503.21006;
- MAPPDFpol1.0: PLB 865 (2025) 139497;
- NNPDFpol2.0: JHEP 07 (2025) 168.

Goal and scope of the present analysis

- Determine polarized proton PDFs from a global analysis of longitudinally polarized inclusive DIS and charge-separated SIDIS data.
- Use a baseline fit built from world fixed-target DIS+SIDIS data only.
- Add projected EIC SIDIS pseudodata for identified $\pi^{\pm}$ and $K^{\pm}$ production at

$$E_e \times E_p = 5 \times 41 \ \mathrm{GeV}^2, \qquad 18 \times 275 \ \mathrm{GeV}^2.$$

- Study:
  - fit quality and stability,
  - dependence on the minimum hadron-energy cut $z_{\min}$,
  - impact on selected helicity PDFs,
  - comparisons to the baseline fit and to recent global determinations,
  - truncated moments relevant to the spin sum-rule discussion.
- Provide the resulting Monte Carlo PDF sets in `LHAPDF` format.

Analysis scope

The analysis is designed to isolate the incremental impact of projected EIC SIDIS data within the same DIS+SIDIS framework.

Leading-twist polarized DIS framework

In leading-twist collinear factorization, the polarized inclusive DIS structure function is written as

$$g_1(x,Q^2) = \frac{1}{2}\sum_q e_q^2 \Big[\Delta q(x,Q^2) \otimes_x \Delta C_q(x,Q^2) + \Delta g(x,Q^2) \otimes_x \Delta C_g(x,Q^2)\Big],$$

with Mellin convolution

$$[f \otimes_x g](x) = \int_x^1 \frac{dy}{y} f(y)\, g\left(\frac{x}{y}\right).$$

- NLO DGLAP evolution in the $\overline{\mathrm{MS}}$ scheme.
- Input scale: $Q_0^2 = 1\ \mathrm{GeV}^2$.
- Zero-mass VFNS used in the present fit; TMC, higher-twist are left for future work.
- Inclusive DIS constrains mainly the quark combinations directly, and Δg through scaling violations.

Practical point

The baseline fit uses the fixed-target polarized DIS data while keeping the theory setup consistent with the SIDIS sector and the EIC pseudodata study.

Polarized SIDIS framework and the observable A_1^h

For identified hadrons in the current fragmentation region,

$$g_1^h(x,z,Q^2) = \frac{1}{2}\sum_q e_q^2 \Big\{ [\Delta q \otimes_x \Delta C_{qq} + \Delta g \otimes_x \Delta C_{qg}] \otimes_z D_q^h + \Delta q \otimes_x \Delta C_{gq} \otimes_z D_g^h \Big\},$$

with

$$[f \otimes_z g](z) = \int_z^1 \frac{d\zeta}{\zeta} f(\zeta)\, g\left(\frac{z}{\zeta}\right), \qquad A_1^h(x,z,Q^2) = \frac{g_1^h(x,z,Q^2)}{F_1^h(x,z,Q^2)}.$$

- NLO SIDIS coefficient functions are used consistently.
- Fragmentation functions: `MAPFF1.0` NLO for charged pions and kaons.
- Charge-separated pions mainly constrain $\Delta\bar{u}$ and $\Delta\bar{d}$.
- Charge-separated kaons provide direct leverage on the strange sector.

Main physics point

SIDIS is the key channel for flavor separation; accordingly, the EIC improvement highlighted in this talk is driven primarily by the identified-hadron asymmetries.

Baseline data set and observables entering the fit

Baseline fit: pDIS+SIDIS base

- Polarized inclusive DIS: EMC, SMC, COMPASS, E142/E143/E154/E155, HERMES, JLab Hall-A, CLAS.
- Polarized SIDIS: HERMES and COMPASS proton/deuteron charge-separated $\pi^{\pm}$ and $K^{\pm}$ asymmetries.
- Common DIS cuts are imposed throughout: $Q^2 \geq 1\ \mathrm{GeV}^2$, $W^2 \geq 4\ \mathrm{GeV}^2$.

Data-set breakdown in the baseline fit

Set	Obs.	N_{dat}	χ^2/N_{dat}
JLab E06-014	g_1^n/F_1^n	4	2.010
JLab E97-103	g_1^n	2	0.414
JLab E99-117	g_1^n/F_1^n	1	0.006
JLab EG1-DVCS	g_1^d/F_1^d	19	0.162
JLab EG1-DVCS	g_1^p/F_1^p	21	0.132
SMC	g_1^d	12	1.315
SMC	g_1^p	12	0.373
COMPASS	g_1^d	15	0.331
COMPASS	g_1^p	17	0.455
HERMES	g_1^n	9	0.226
HERMES	g_1^d	15	1.197
HERMES	g_1^p	15	1.005

Data-set breakdown in the baseline fit

Set	Obs.	N_{dat}	χ^2/N_{dat}
COMPASS	$A_1^p(K^-)$	12	0.727
COMPASS	$A_1^p(K^+)$	12	0.719
COMPASS	$A_1^p(\pi^-)$	12	1.201
COMPASS	$A_1^p(\pi^+)$	12	2.500
COMPASS	$A_1^d(K^-)$	10	0.891
COMPASS	$A_1^d(K^+)$	10	0.321
COMPASS	$A_1^d(\pi^-)$	10	0.448
COMPASS	$A_1^d(\pi^+)$	10	0.320
HERMES	$A_1^d(K^-)$	9	0.612
HERMES	$A_1^d(K^+)$	9	1.459
HERMES	$A_1^d(\pi^-)$	9	1.265
HERMES	$A_1^d(\pi^+)$	9	0.334
HERMES	$A_1^p(\pi^-)$	9	1.103
HERMES	$A_1^p(\pi^+)$	9	1.889
E142	g_1^n	8	0.714
E143	g_1^d	27	1.315
E143	g_1^p	27	0.902
E154	g_1^n	11	0.324
E155	g_1^p/F_1^p	24	0.630
E155	g_1^n/F_1^n	24	0.644
EMC	g_1^p	10	0.639

Data-set breakdown in the baseline fit

		N_{dat}	χ^2/N_{dat}
Total	pDIS+SIDIS base	415	0.727

ECCE detector design and projected polarized SIDIS asymmetries

ECCE-based SIDIS study

The projected SIDIS input is based on the EIC Comprehensive Chromodynamics Experiment (ECCE) detector-design study for longitudinal double-spin asymmetries in $ep \to e' hX$.

Detector-level simulation

Unpolarized SIDIS events are generated with PYTHIA-6 and passed through a full GEANT simulation of the ECCE detector concept, including reconstruction effects.

Beam configurations

The two configurations used in this analysis,

$$E_e \times E_p = 5 \times 41, \qquad 18 \times 275 \ \mathrm{GeV}^2,$$

probe complementary regions of the SIDIS (x, Q^2, z) phase space.

From unpolarized MC to spin asymmetries

Since the generated events are unpolarized, helicity-dependent weights are applied at parton level using polarized PDFs (DSSV14) and FFs (DSS):

$$w \sim 1 + \lambda \, D(y) \, \frac{\Delta f \otimes D^h_{q,g}}{F^h_{UU}}.$$

This produces projected $A_1^h(x, z, Q^2)$ asymmetries for identified hadrons.

Measured hadron channels

The detector study provides projected asymmetries for charge-separated pion and kaon production:

$$h = \pi^+, \ \pi^-, \ K^+, \ K^-.$$

Pions drive light-sea separation; kaons provide the strange-sector lever arm.

Why this matters for the fit

The ECCE study [Nucl. Instrum. Meth. A 1056 (2023) 168563; Nucl. Instrum. Meth. A 1073 (2025) 170240] finds limited detector smearing, good acceptance, and broad kinematic coverage, making the projected SIDIS asymmetries suitable for precision helicity-PDF impact studies.

Projected EIC SIDIS pseudodata and event selections

The projected EIC input follows the ECCE-based detector-level SIDIS study: we use its kinematic coverage, binning, and projected uncertainties to build pseudodata for

$$A_1^{p,h}(x, z, Q^2), \qquad h = \pi^+, \pi^-, K^+, K^-.$$

- Projected ECCE uncertainties: $\mathcal{L}_{\rm int} = 10\ \mathrm{fb}^{-1}$, $P_e = P_p = 70\%$; bin-by-bin uncorrelated statistical/detector errors plus a fully correlated global 2% beam-polarization scale uncertainty.
- Beam-energy configurations:

$$5 \times 41\ \mathrm{GeV}^2 \quad \text{and} \quad 18 \times 275\ \mathrm{GeV}^2.$$

- Polarized DIS-region selections in the simulation setup include
  - $Q^2 \geq 1\ \mathrm{GeV}^2$,
  - $W^2 \geq 4\ \mathrm{GeV}^2$,
- Central pseudodata are generated from the baseline NLO theory using our fitted `pDIS+SIDIS` polarized PDFs, `NNPDF4.0` unpolarized PDFs, and `MAPFF1.0` FFs.

`MontBlanc/Denali` framework

The projected EIC pseudodata are generated and fitted within the same NLO DIS+SIDIS framework, using the `MontBlanc/Denali` framework [Phys. Lett. B 865 (2025) 139497].

Kinematic coverage: world data plus projected EIC reach

- Triangles denote current polarized DIS data, while squares denote current polarized SIDIS measurements.
- Circles and stars denote projected EIC SIDIS asymmetries for $\pi^{\pm}$ and $K^{\pm}$ at the 5×41 and 18×275 GeV^2 beam configurations, respectively.
- The EIC extends the accessible SIDIS phase space to much lower x and substantially broader Q^2.
- The main gain is not only a larger number of points, but also a qualitatively stronger lever arm in both x and Q^2.
- The EIC improvement is not merely statistical: it opens a qualitatively new kinematic domain, especially toward small x, where present constraints are weakest.

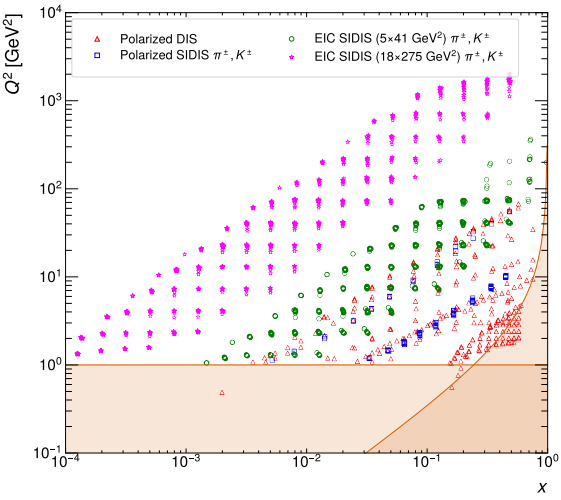

World polarized DIS and SIDIS coverage compared with the projected EIC SIDIS reach for the 5×41 GeV^2 and 18×275 GeV^2 beam configurations.

Fitting methodology: neural networks, Monte Carlo replicas, positivity

- The QCD fit is performed using the `MontBlanc/Denali` setup, following Ref. [Phys. Lett. B 865 (2025) 139497].
- Experimental uncertainties are propagated through a Monte Carlo replica ensemble.
- At $Q_0^2 = 1\ \mathrm{GeV}^2$, the independent flavor basis is

$$\{\Delta f_u, \Delta f_{\bar{u}}, \Delta f_d, \Delta f_{\bar{d}}, \Delta f_s, \Delta f_{\bar{s}}, \Delta f_g\}.$$

- Positivity is imposed by construction at the parametrization scale,

$$\Delta f_i^{(k)}(x, Q_0^2) = \left[2\,\mathrm{NN}_i(x) - 1\right] f_i^{(r_k)}(x, Q_0^2),$$

  using replicas of the unpolarized input set.
- External inputs: `NNPDF4.0` NLO for unpolarized PDFs and `MAPFF1.0` NLO for FFs.

Main message

The methodology propagates not only the experimental uncertainties, but also the uncertainty associated with the external unpolarized PDF and FF inputs.

$z_{\min}$ dependence and χ^2 stability

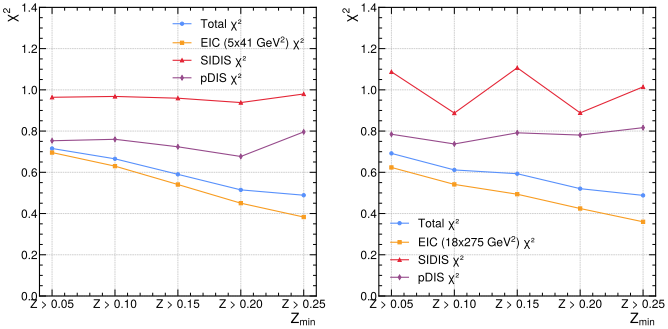

- For both beam configurations the total χ^2 shows a smooth dependence on $z_{\min}$.
- Polarized DIS and SIDIS partial contributions remain stable across the scan.
- A mild preference emerges for the more conservative selection $z_{\min} > 0.2$.

Central result

We therefore adopt $z_{\min} > 0.2$ as the default, while also showing $z_{\min} > 0.1$ to assess the sensitivity to the hadron-energy cut.

Dataset-by-dataset stability: baseline vs EIC-augmented fits

- Blue denotes the baseline pDIS+SIDIS fit, while red denotes the EIC-augmented fit.
- Adding projected EIC pseudodata does not spoil the description of the existing fixed-target measurements.
- The changes in the partial χ^2 values are generally modest and fluctuate around the baseline results.
- This suggests a stable incorporation of the projected EIC pseudodata, with no visible deterioration in the description of the existing polarized DIS and SIDIS data.

Methodological point

The projected EIC pseudodata are incorporated within the same DIS+SIDIS framework, while preserving a stable description of the existing fixed-target world data.

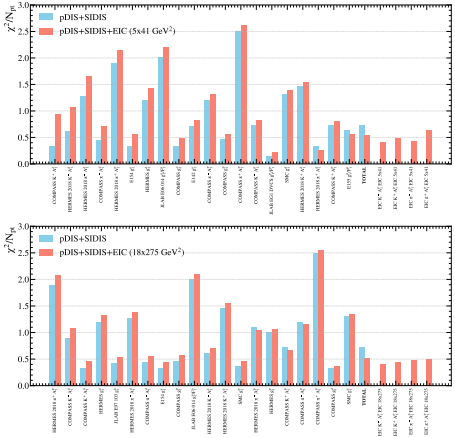

Dataset-by-dataset comparison of partial χ^2 values for the baseline and EIC-augmented fits, shown for the 5×41 and 18×275 EIC configurations.

Impact of EIC pseudodata at 5×41 GeV^2

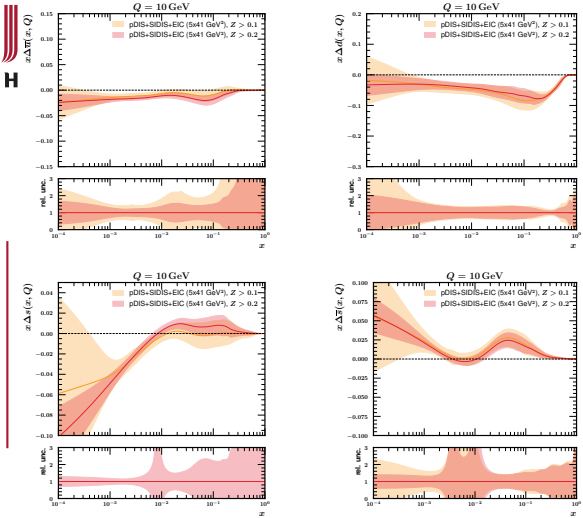

Comparison of helicity PDFs obtained with $z_{\min} > 0.1$ and $z_{\min} > 0.2$ for the 5×41 EIC configuration at $Q^2 = 100$ GeV^2: $\Delta\bar{u}$, Δd, Δs, and $\Delta\bar{s}$.

- The central values are broadly consistent between the $z_{\min} > 0.1$ and $z_{\min} > 0.2$ choices.
- The more conservative $z_{\min} > 0.2$ cut typically yields smoother and somewhat tighter uncertainty bands.
- The most visible effect is seen in SIDIS-sensitive sea-quark distributions and, indirectly, in the gluon sector through evolution and correlations.
- This indicates that the main physics conclusions are stable against reasonable variations of the hadron-energy cut.

Central result

At 5×41, the EIC pseudodata already provide visible improvements in SIDIS-sensitive sea-quark helicity PDFs, while the comparison of $z_{\min}$ choices confirms the stability of the extraction.

Comparison to the baseline pDIS+SIDIS fit

- The EIC-augmented fit mainly reduces uncertainties in regions where the baseline fit is extrapolation-dominated.
- The strongest gain is seen in SIDIS-sensitive sea-quark helicity PDFs, especially $\Delta\bar{u}$, $\Delta\bar{d}$, and $\Delta\bar{s}$.
- Δg also improves indirectly through the larger evolution lever arm at small x.
- Overall, the projected EIC input makes the low-x helicity sector significantly more data-driven within the present NLO DIS+SIDIS framework.

Main physics point

Projected EIC SIDIS data substantially sharpen the sea-quark helicity sector, while also improving the small-x gluon uncertainty indirectly through QCD evolution.

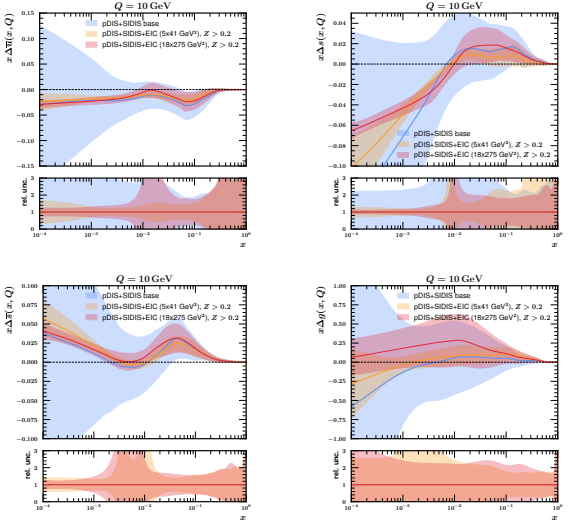

Baseline vs EIC-augmented helicity PDFs at $Q^2 = 100\ \mathrm{GeV}^2$ for $\Delta\bar{u}$, $\Delta\bar{d}$, $\Delta\bar{s}$, and Δg.

Comparison with MAPPDFpol1.0 (NLO set)

- Overall agreement in the data-constrained region provides a non-trivial cross-check of our baseline methodology.
- Differences at medium-to-small x are expected, since our fit includes projected EIC SIDIS pseudodata.
- The comparison is especially informative in the sea-quark sector, where both analyses rely on neural-network Monte Carlo methodologies.
- The EIC input mainly translates into narrower uncertainty bands in regions that remain only weakly constrained by current data.

Key result

The comparison with MAPPDFpol1.0NLO shows broad consistency in the data-driven region, while the projected EIC SIDIS input leads to a visibly improved determination of the sea-quark helicity PDFs at lower x.

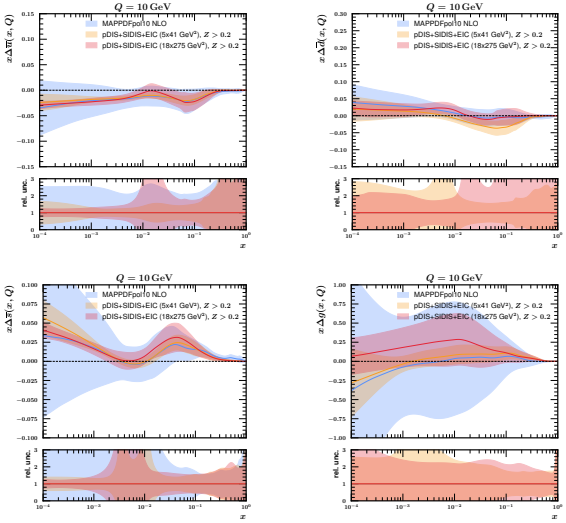

Comparison with MAPPDFpol1.0NLO at $Q^2 = 100\ \mathrm{GeV}^2$ for $\Delta\bar{u}$, $\Delta\bar{d}$, $\Delta\bar{s}$, and Δg.

Comparison with NNPDFpol2.0

- NNPDFpol2.0 provides an important modern global benchmark; here we compare to its NLO member for consistency with our NLO DIS+SIDIS setup.
- Our analysis combines charge-identified SIDIS asymmetries from HERMES and COMPASS with projected EIC SIDIS pseudodata.
- This leads to particularly visible differences in the strange sector and in SIDIS-driven light-sea flavor separation.
- The comparison highlights the added value of direct SIDIS information for constraining sea-quark helicity PDFs.

Key result

Relative to NNPDFpol2.0, the inclusion of charge-separated SIDIS data and projected EIC measurements leads to visibly stronger constraints in the strange and light-sea helicity sectors.

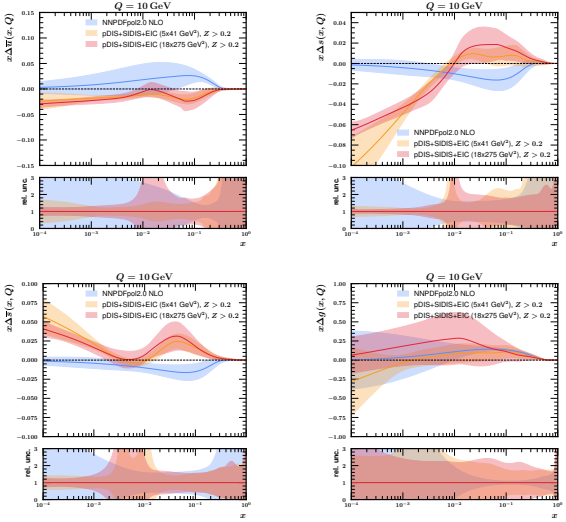

Comparison with NNPDFpol2.0 at $Q^2 = 100\ \mathrm{GeV}^2$: $\Delta\bar{u}$, $\Delta\bar{d}$, $\Delta\bar{s}$, and Δg.

Truncated moments and the low-x spin contribution

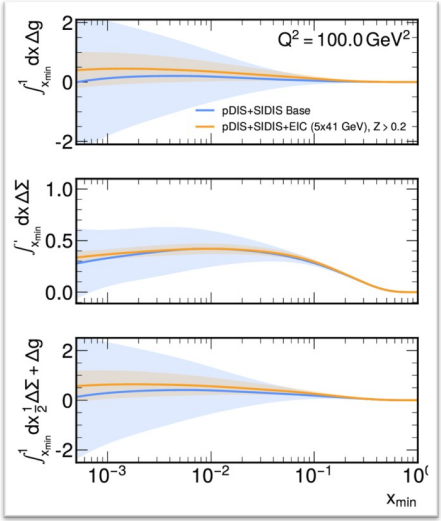

Truncated moments of Δg, $\Delta\Sigma$, and $\frac{1}{2}\Delta\Sigma + \Delta g$ at $Q^2 = 100\ \mathrm{GeV}^2$ as functions of x_{min}.

- We study the truncated moments of Δg, $\Delta\Sigma$, and $\frac{1}{2}\Delta\Sigma + \Delta g$ as functions of x_{min}.
- In the baseline fit, the uncertainties grow rapidly as x_{min} is lowered.
- The projected EIC pseudodata significantly reduce the uncertainty bands for both quark and gluon contributions, especially as the integration is extended into the small-x region.
- This directly improves the stability of the quark-plus-gluon spin contribution in the poorly constrained low-x region.

Main physics point

The projected EIC input is highly relevant for proton-spin phenomenology because it reduces the small-x uncertainty in the quark-plus-gluon helicity contribution.

Projected EIC impact relative to existing fixed-target SIDIS data

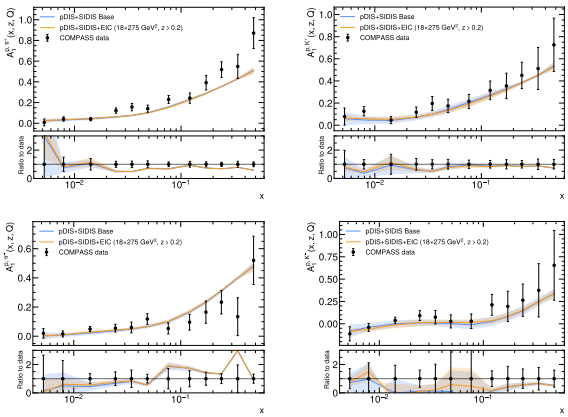

Comparison of baseline and EIC-augmented predictions with COMPASS $A_1^{p,h}$ asymmetries for π^+, K^+, π^-, and K^-.

- The inclusion of projected EIC input leaves the description of the COMPASS asymmetries essentially unchanged.
- The main visible effect is not a shift of the central values, but rather a tightening of the uncertainty bands in the small-x region.
- This suggests that the projected EIC pseudodata mainly improve the precision of the determination, while leaving the fixed-target SIDIS description stable.
- In this sense, the projected EIC input acts primarily as a precision lever, rather than as a source of distortion of the existing SIDIS phenomenology.

Main physics point

The projected EIC input acts mainly as a precision lever, tightening the helicity-PDF uncertainties without materially changing the fitted fixed-target SIDIS description.

Main conclusions and outlook

- We presented a new NLO global determination of polarized proton PDFs from inclusive DIS and charge-separated SIDIS data.
- Projected EIC SIDIS pseudodata at 5 $\mathrm{GeV} \times 41\ \mathrm{GeV}$ and 18 $\mathrm{GeV} \times 275\ \mathrm{GeV}$ extend the accessible (x, Q^2) region, reaching down to about $x \sim 10^{-5}$.
- The largest projected impact is on sea-quark flavor separation and on the small-x uncertainty of Δg, the latter mainly through the extended Q^2 evolution lever arm.
- The EIC-augmented fits remain stable, with controlled $z_{\min}$ dependence and no visible deterioration of the existing DIS+SIDIS description.
- Charge-identified SIDIS observables are central to the improvement, providing FF-dependent flavor sensitivity to the light sea and strange sector.
- Truncated moments show reduced uncertainty in the low-x contribution to $\frac{1}{2}\Delta\Sigma + \Delta g$.
- The resulting Monte Carlo PDF sets are released in LHAPDF format.

Main conclusion

Projected EIC SIDIS measurements can transform polarized-PDF phenomenology by turning the small-x and sea-flavor sectors from extrapolation-dominated to substantially more data-driven.

THANK
YOU!

Availability of the resulting PDF sets: HAPS-pPDF1.0

Public delivery

The polarized PDFs extracted in this analysis are released in standard LHAPDF format as Monte Carlo replica ensembles.

- Separate sets are provided for the baseline fit and the EIC-augmented scenarios.
- Central values are computed as replica averages; uncertainties follow from replica statistics.
- The public grids are released through the HAPS Collaboration (Hadron and Partonic Structure Collaboration) repository, providing the HAPS-pPDF1.0 Monte Carlo replica sets.

https://github.com/HAPS-Collaboration/HAPS-pPDF1.0

Natural next steps

More complete FF uncertainty propagation, higher-order SIDIS corrections, and broader polarized processes will make the EIC program even more powerful.

Backup: scope and theory-systematics caveats

What is included in the present analysis

- NLO leading-twist DIS+SIDIS framework with DGLAP evolution.
- Fixed-target polarized DIS+SIDIS baseline, plus projected EIC SIDIS pseudodata.
- Neural-network parametrization, Monte Carlo replicas, and positivity at the input scale.
- External inputs: NNPDF4.0 unpolarized PDFs and MAPFF1.0 FFs.

What is left for future extensions

- Full NNLO SIDIS treatment and associated theory-systematics studies.
- More complete FF uncertainty propagation, especially for kaon channels.
- Target-mass, higher-twist, and nuclear corrections in low-W^2 / high-x regions.
- Inclusion of polarized RHIC pp data to combine SIDIS flavor sensitivity with direct collider constraints on Δg.

Representative proton SIDIS asymmetries: pion channels

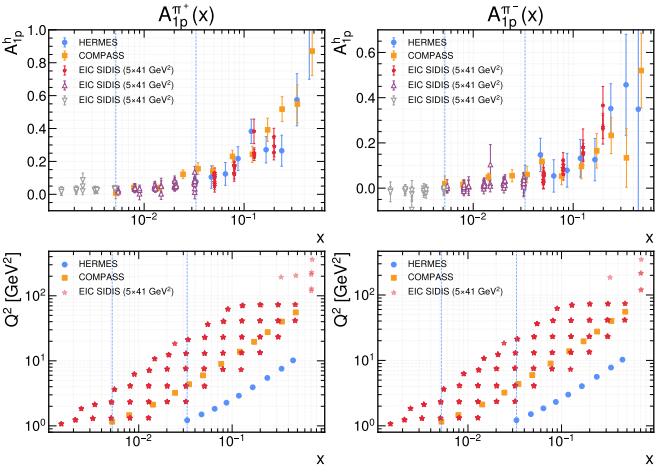

- Projected EIC A_1^{p,π^+} and A_1^{p,π^-} connect smoothly to the fixed-target region.
- The gain is strongest in the low-x region and over a broader Q^2 range than HERMES/COMPASS.
- The pion channels are the main drivers for improved light-sea flavor separation.

Representative proton SIDIS asymmetries: kaon channels

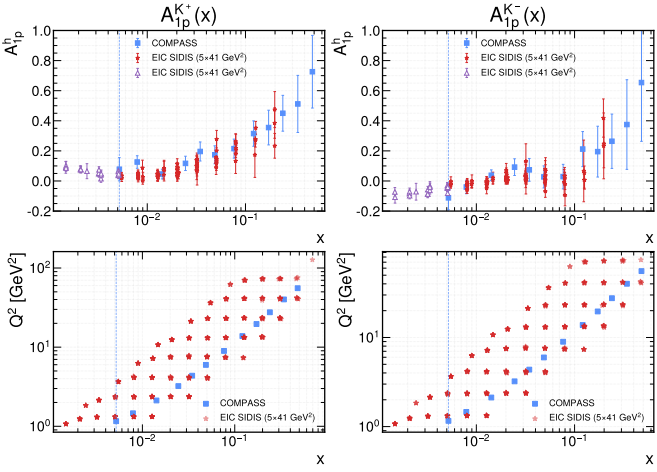

- The EIC kaon asymmetries dramatically extend the strange-sensitive SIDIS region.
- This is the crucial ingredient for improving constraints on Δs and $\Delta\bar{s}$.
- The interpretation remains linked to FF input, which is why consistent NLO SIDIS+FF treatment is important.

Impact of EIC pseudodata at 18×275 GeV^2

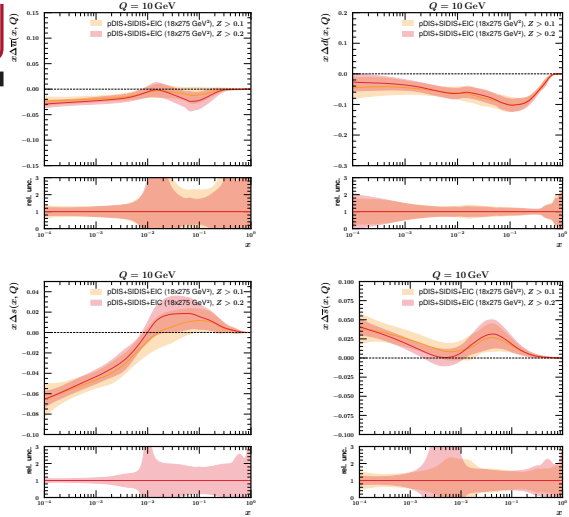

Comparison of helicity PDFs obtained with $z_{\min} > 0.1$ and $z_{\min} > 0.2$ for the 18×275 EIC configuration at $Q^2 = 100$ GeV^2: $\Delta\bar{u}$, Δd, Δs, and $\Delta\bar{s}$.

- The higher-energy configuration extends the reach further into the small-x region.
- The same stability pattern with respect to the $z_{\min}$ choice is observed.
- The improvement is strongest in the regions where current data provide the least direct leverage.
- Relative to the lower-energy setup, the 18×275 configuration more clearly strengthens the small-x constraints.

Central result

Relative to 5×41, the 18×275 configuration most clearly strengthens the small-x constraints.